Tuijin Jishu/Journal of Propulsion Technology
ISSN: 1001-4055
Vol. 45 No. 2 (2024)

Comparing Rectangular and Circular Patch Antennas for 5G Deployment at 28 Ghz

Ibrahim Khouyaoui[1], Mohamed Hamdaoui[2], Mouhssine Elbathaoui[3], Jaouad Foshi[4]

[1]*Electronics Instrumentation and Intelligent Systems Team, ER2TI Laboratory, Department of Physics, Faculty of Sciences and Technics, Moulay Ismail University of Meknes, Errachidia Morocco*

[2]*Electronics Instrumentation and Intelligent Systems Team, ER2TI Laboratory, Department of Physics, Faculty of Sciences and Technics, Errachidia, Moulay Ismail University of Meknes, Morocco*

Abstract: - This research paper elucidates the methodological framework and performance analysis of microstrip patch antennas tailored for 5G wireless communication systems. The proposed antenna configurations encompass a standalone rectangular patch antenna, a circular patch antenna, and an array of patch elements. Employing Rogers RT 5880 substrate material with a thickness of 0.254 mm and operating at a frequency of 28 GHz, these antennas are meticulously crafted. Simulation results, facilitated by the CST Studio Suite software, encompass key parameters such as S11, voltage standing wave ratio (VSWR), radiation pattern, gain, and efficiency. Analysis of these results reveals that the individual circular antenna design resonates at 28 GHz with a return loss of -36.2 dB, exhibiting a bandwidth of 8.6 GHz, a gain of 3.61 dBi, and an efficiency of 92%. Conversely, the single rectangular antenna design operates at the same resonance frequency with a return loss of -56.6 dB, offering a bandwidth exceeding 9.6 GHz, a gain surpassing 9.6 dBi, and an efficiency of 91%. Further examination of array configurations reveals that the 2x1 circular antenna design resonates at 28 GHz with a return loss of -50.6 dB, presenting a bandwidth of 6.5 GHz, a gain of 7.06 dBi, and an efficiency of 93%. Conversely, the 2x1 rectangular antenna design spans a resonance frequency range from 24 GHz to 28 GHz, achieving a return loss between -32 dB to -54.5 dB, and a bandwidth surpassing 12.6 GHz. It attains a higher gain of 7.2 dBi with an efficiency exceeding 93%. Analysis of the 4x1 configurations unveils that the circular antenna design resonates at 28 GHz with a return loss of -35 dB, offering a bandwidth of 8 GHz, a gain of 9.05 dBi, and an efficiency of 95%. Conversely, the 4x1 rectangular antenna design operates within a resonance frequency range from 21.5 GHz to 27.9 GHz, exhibiting a return loss varying from -27 dB to -61 dB, and a bandwidth spanning from 2.1 GHz to 9.3 GHz. This configuration achieves a gain of 9.04 dBi with an efficiency surpassing 94%.

Keywords*: Rectangular and circular patch, array antenna, partial ground, S11.*

1. Introduction

In the current context, increasing needs and widespread use of wireless communication devices in various sectors such as medicine, defence, and aerospace are driving manufacturers to constantly innovate in the field of wireless communication systems. Over the years, technological advancements have been particularly significant in the field of microwave circuits. The importance of antennas in the communication chain has grown, posing additional challenges in terms of installation in constrained spaces. [1] [3] [6] [25] [29] [30] Microstrip and patch antennas are now essential components of fifth-generation (5G) wireless communications, due to their characteristics such as compactness, low cost, and ease of integration into various electronic equipment, satellites, vehicles, and aircraft, both inside and outside the human body. [1-4] However, these antennas have performance limitations such as narrow bandwidth, low reception power, and relatively low gain, restricting their use in certain scenarios. 5G wireless communication technology utilizes high frequencies that heavily depend on antenna performance, particularly in terms of reflection, gain, and bandwidth. [7] [8] [29] [30] To address these challenges and meet user needs, it is crucial to design and produce antennas that offer optimal performance in terms of gain, reflection, and bandwidth. [31] [32]

Faced with the surge in demand for wireless communication, 4G technology is reaching saturation. [9] [10]5G emerges as the indispensable solution to address these growing needs, offering blazing speeds, expanded coverage, and minimal latency. 5G promises a maximum data rate of 10 Gbps, a hundred times faster than 4G, enabling instant and seamless data transfers. [1] [11] [12] For smart cities and the Internet of Things (IoT), 5G provides massive connectivity capacity, supporting up to a million devices per square kilometer. Moreover, its network capacity of 10 Tbps per square kilometer ensures efficient management of simultaneous connections. Finally, its low latency, less than one millisecond, is essential for real-time applications like virtual reality and remote surgery. To fully harness the potential of 5G, the use of higher frequencies is necessary. [13] [14] [15] The International Telecommunication Union (ITU) has defined specific frequency bands for 5G, including between 3.4 and 3.6 GHz, 5 and 6 GHz, 24.25 and 27.5 GHz, 37 and 40.5 GHz, and 66 and 76 GHz. The FCC has also allocated the 27.5 to 28.35 GHz band for 5G. In this study, we focus on the 28 GHz band, which offers distinct advantages for 5G. [16-20] This band provides an optimal compromise between capacity and propagation, enabling efficient deployment and extensive coverage. Furthermore, it is already being used for experimental purposes in several countries, facilitating its adoption and standardization.5G, with its revolutionary features, is poised to transform the landscape of wireless communications. The 28 GHz band plays a crucial role in realizing its full potential, offering an ideal combination of data rate, coverage, and latency to meet the growing demands for connectivity. [25] The requirements imposed on 5G antennas are particularly stringent, given the performance needed to support high data rates and carrier frequencies of this emerging technology. Among the key characteristics of 5G antennas, wide bandwidth is crucial to ensure support for the extended data channels inherent to 5G. Additionally, high directivity is essential to concentrate signals towards target users, thereby reducing unwanted interference. High gain is also required to compensate for propagation losses at the high carrier frequencies characteristic of 5G. Furthermore, compact size and lightweight are essential to facilitate the integration of antennas into base stations and mobile terminals. It is also crucial for these antennas to exhibit mechanical robustness, allowing them to withstand the most challenging environmental conditions, while remaining affordable for widespread deployment of 5G. [25-35]

In this context, microstrip patch antennas emerge as a promising solution for 5G. Their simple design, economical fabrication, and ability to integrate advanced features make them an attractive choice for a variety of 5G applications. Research on 5G antennas focuses on several major challenges. It is crucial to develop antennas with even wider bandwidths to support the future evolutions of 5G. Additionally, improving the energy efficiency of antennas to minimize the energy consumption of 5G networks is essential. Integrating features such as MIMO and beamforming into multifunctional antennas is also a significant research direction. Finally, reducing the cost of 5G antennas is indispensable to promote their widespread adoption. The constant evolution of wireless communication standards places antenna research in a cycle of continuous development. Each new generation of standards brings increasingly complex challenges, requiring antennas to be ever more efficient and innovative to meet the growing demands of wireless connectivity. [25]

Research and design of antennas for the 5G millimetre-wave band, particularly in the 28 GHz frequency range, are active areas of investigation. Although this band offers promising prospects for 5G, it also presents significant challenges in antenna design. Various types of antennas have been studied for 5G at 28 GHz, each exhibiting varying performance: Antenna [22]: Operating at a frequency of 28 GHz, this antenna exhibits a gain of 7.47 dB and a bandwidth of 4.63 GHz. However, it has a return loss of -30.70 dB, which is insufficient for integration into 5G applications. Antenna [23]: Considered inadequate for 5G applications, it offers a maximum gain of 3.7 dBi and a return loss of -35 db. Antenna arrays [24]: These antennas display a gain of 8.42 dB and a compact size, but are not suitable for 5G applications due to their narrow bandwidth and low return loss. Printed antenna [25]: With a gain of 9.42 dBi, it is characterized by a large size, a narrow bandwidth of 1.43 GHz, and a return loss of -35.91 dB, making it inappropriate for 5G applications. Printed antenna array [26]: Possessing a maximum directivity of 6.9 dBi, its insufficient return loss of -17 dB makes its use challenging for 5G. Antenna array [27]: With a maximum directivity of 9.87 dBi, its bandwidth of 2.68 GHz is considered low, and its return loss of -30.71 dB makes its use challenging for 5G applications. Antenna array [28]: Although it has a maximum gain of 4.78 dBi, its bandwidth of 0.55 GHz is very low, and its return loss of -25 dB is insufficient for 5G applications, in addition to having a costly design. Despite these efforts, the demand for compact and high-performance 5G antennas remains high. In our research, we present a comparison between a rectangular and circular microstrip antenna array of 4 elements, with a partial ground plane featuring a central square slot, optimized using CST software.

The rectangular antenna array offers a wide bandwidth of 9.3 GHz, a maximum gain of 9.4 dB, and a return loss of -61 dBi. However, the circular antenna array offers a wide bandwidth of 8 GHz, a maximum gain of 9.05 dB, and a return loss of -35 dBi. [25] [29] [30].

This article is structured into several stages. Firstly, we designed a single rectangular microstrip patch antenna operating at 28 GHz. Next, we developed and simulated a single rectangular and circular microstrip patch antenna element, incorporating partial modification of the ground plane to enhance its performance at the same frequency. Additionally, we designed and simulated 2x1 arrays of rectangular and circular microstrip patch antennas to optimize their gain. Finally, 4x1 arrays of rectangular and circular microstrip patch antennas were also developed and simulated to further explore performance enhancement possibilities in the context of 5G wireless communication. These contributions represent a significant advancement in the field of microstrip antennas for fifth-generation communication systems.

2. Objectives simple rectangular MPA using Mathematical equation

The design of the proposed array antenna for 5G wireless applications is initiated by the design of a single rectangular patch antenna. The single antenna element is made up patch of rectangular shaped with an impedance of 50 Ω transmission line. The reason that 50 Ω is utilized in transmission lines is because it is the most common in order to reduce the amount of reflection and return loss. With this particular configuration, the radiating patch of the single patch antenna is constructed out of copper that has a thickness of 0.035 millimeters. Copper is also employed as a conducting material in the antenna's ground plane and transmission line. Roggers RT 5880 also used as a substrate material with a standard thickness of 0.254 mm. Moreover, the operating frequency of this suggested single rectangular patch antenna is 28 GHz.

Following equations from (1--7), an antenna of single element is designed operating at 28 GHz. Simple microstrip patch antenna at 28 GHz is depicted in figure 1. The simulated reflection co-efficient of proposed single design with dimensions are shown in figure 2. The calculated and optimized table are listed in table 1.

Using formulas (1-- 7), the single antenna element is designed. [1] [29] [30]

Rectangular patch antenna width

$$W = \frac{c}{f_0}\sqrt{\frac{2}{\epsilon_r+1}} = 4.23 \text{ mm} \quad (1)$$

$$\epsilon_{eff} = \frac{\varepsilon_R+1}{2} + \frac{\varepsilon_R-1}{2}\left[\frac{1}{\sqrt{1+12\frac{h}{w}}}\right] \quad (2)$$

$$\epsilon_{eff} = \frac{2.2+1}{2} + \frac{2.2-1}{2}\left[\frac{1}{\sqrt{1+12\frac{0.254}{4.23}}}\right] = 2.05$$

Rectangular patch antenna length

$$L = \frac{c}{2f_0\sqrt{\epsilon_{eff}}} - 0.842h\frac{(\epsilon_{eff}+0.3)(\frac{W}{h}+0.264)}{(\epsilon_{eff}-0.258)(\frac{W}{h}+0.8)} \quad (3)$$

$$L = \frac{3}{2\,x280\sqrt{2.05}} - 0.842x0.254\frac{(2.05+0.3)(\frac{4.23}{0.254}+0.264)}{(2.05-0.258)(\frac{4.23}{0.254}+0.8)} = 3.466\text{mm}$$

Because of fringing fields the length is changed and is assumed by:

$$\frac{\Delta L}{h} = 0.412\frac{(\epsilon_{eff}+0.3)(\frac{W}{h}+0.264)}{(\epsilon_{eff}-0.258)(\frac{W}{h}+0.8)} \quad (4)$$

$$\Delta L = 0.254\left[0.412\frac{(2.05+0.3)(\frac{4.23}{0.254}+0.264)}{(2.05-0.258)(\frac{4.23}{0.254}+0.8)}\right] = 0.523$$

The Effective length L*eff* of patch is:

$$L_{eff} = L + 2\Delta L = 3.466 + 2 * 0.523 = 4.5 \text{ mm} \quad (5)$$

The substrate length (Ls) and width (Ws) are:

$$W_s = 6h + W_p = 6x0.254 + 4.23 = 5.75 \text{ mm} \quad (6)$$

$$L = 6h + L_p = 6 * 0.254 + 3.466 = 5 \text{ mm} \quad (7)$$

Tapez une équation ici.

Table 1. Parameters of initial Rectangular Patch Design

Parameter	Calculated value (mm)	Optimized Values
F_r	28 GHz	--
Patch Width (Wp)	4.23	4.235
Patch Length (Lp)	3.466	3.41
Feed width (wf)	0.74	0.8
Feed Length (Lf)	3.74	3.26
Length of substrate (Ls)	5	8
Width of substrate (Ws)	5.75	8
Inset feed (fi)	1.2	1.1

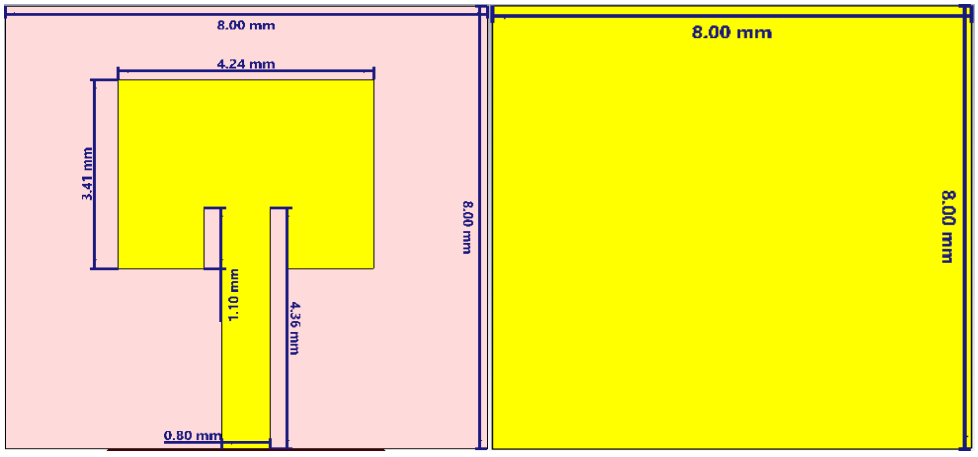

(a) (b)

Figure 1. Simple rectangular Microstrip patch antenna: (a) top view and (b) bottom view

Simulated S11 of proposed simple microstrip patch antenna are depicted in figure 2(a). From the figure, it is shown that it has an impedance of -28.9 at 28 GHz with an impedance bandwidth of 0.6 GHz resonating from 27.6—28.3 GHz. The VSWR are 1.07 below 2dB. In order to improve the bandwidth and other performances, a simple microstrip patch antenna is modified to partial ground with metallic strip extension. [6]- [12]

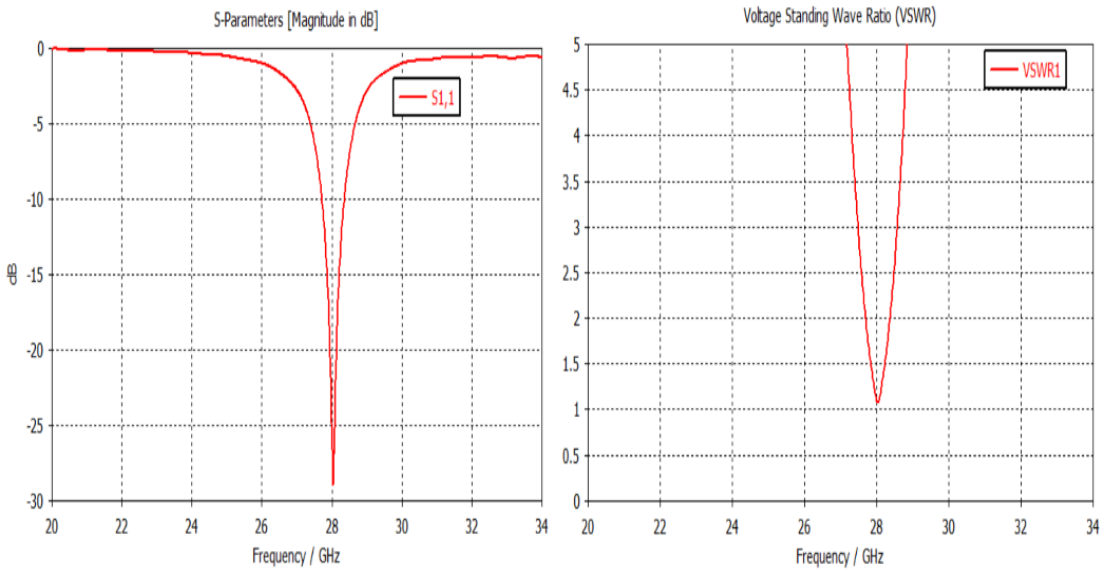

(a) (b)

Figure 2. Simulated results :(a) Return loss (b) VSWR

2.1 Improved rectangular microstrip patch Antenna

Using mathematical equation approach, a simple microstrip are design as described in previous section. This section explains the most compact and modified antenna in order to improve impedance bandwidth, efficiency and gain and other performances. In order to improve the performance of simple microstrip patch Antenna, a truncation ground also known as partial ground are utilized for bandwidth enhancement to fulfill the 5G requirements. Moreover, a rectangular slot is introduced in the mid of partial ground of 1.38 x 1.3 mm^2 dimension and extra vertical strip at the top right corner of partial ground. The top and bottom view of improved single antenna element are depicted in fig 3 (a) and (b) respectively. Using optimization, the labeled values are finalized for improving performance. The simple and optimized improved dimension of rectangular microstrip patch is listed in table 2 as a comparison table. [6]

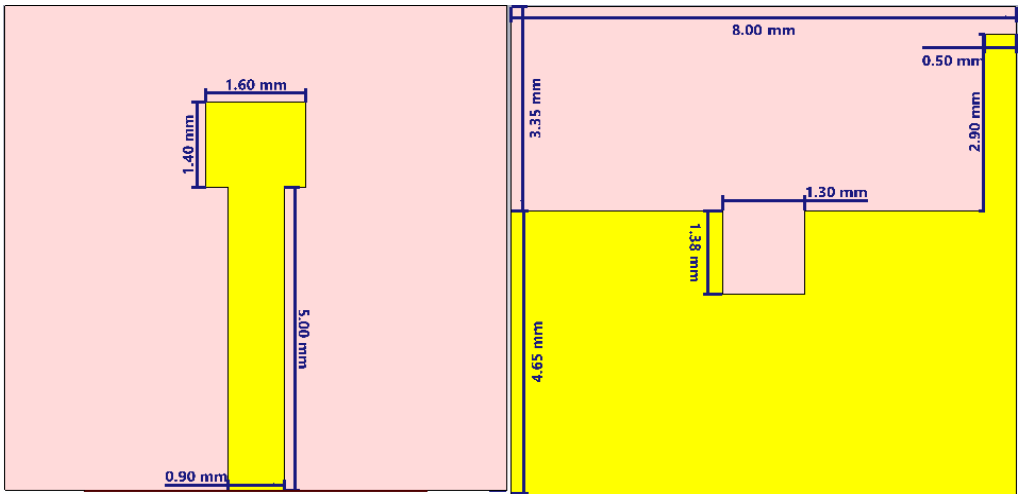

(a) (b)

Figure 3. Single antenna element: (a) Top view and (b) Bottom view

Table 2. Parameter comparison of initial Rectangular Patch Design with Optimized Design

Parameter	Calculated value (mm)	Improved/optimised Design Values(mm)
F_r	28 GHz	--
Patch Width (Wp)	4.23	1.6
Patch Length (Lp)	3.466	1.4
Feed width (wf)	0.74	0.9
Feed Length (Lf)	3.74	5.1
Length of substrate (Ls)	5	8
Width of substrate (Ws)	5.75	8

Figure 4(a) displays the return loss result for the simple MPA and optimised antenna. At resonance frequency of 28 GHz , the optimised antenna element has a reflection co-efficient of -56.6 dB. The operting band of single antenna element is 25.69 -- >34 GHz having a bandiwdth more than 8GHz, which indicated that the optimised antenna has much more improved results as previous simple MPA as depicted in figure 2 (a). Figure 4 (b) predicts the VSWR of optimised patch element. From the figre it is shown than VSWR is below the 2 dB throughout the operating band, which shows the anenna performance well. However, the results proves that the optimised antenna has better performances than simple calculated MPA. [6]

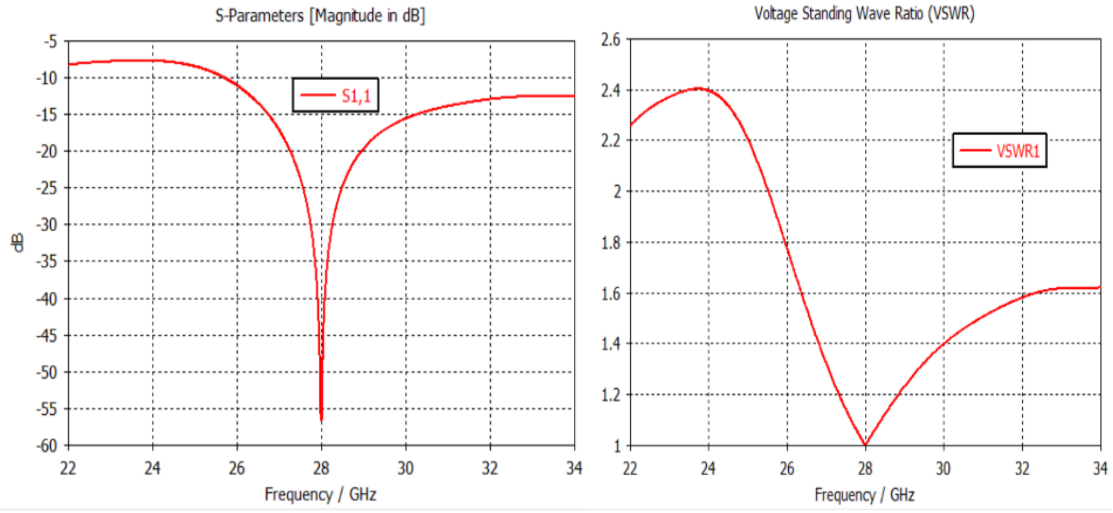

(a) (b)

Figure 4. (a) S11 of proposed optimized single antenna element and (b) VSWR

Figure 5 shows the 2-D & 3-D radiation pattern of the proposed single antenna element. Maximum power is orthogonal to the patch, indicating a directed radiation pattern. Gain of single antenna element is about to 3.59 dBi. Figure 6 (a) shows gain vs frequency plot while 6 (b) indicates eficiency vs frequency. Peak gain of 4 dBi is achived. Efficiency of proposed design is 92 % at lower operating band while more than 91 % at higher operating band.

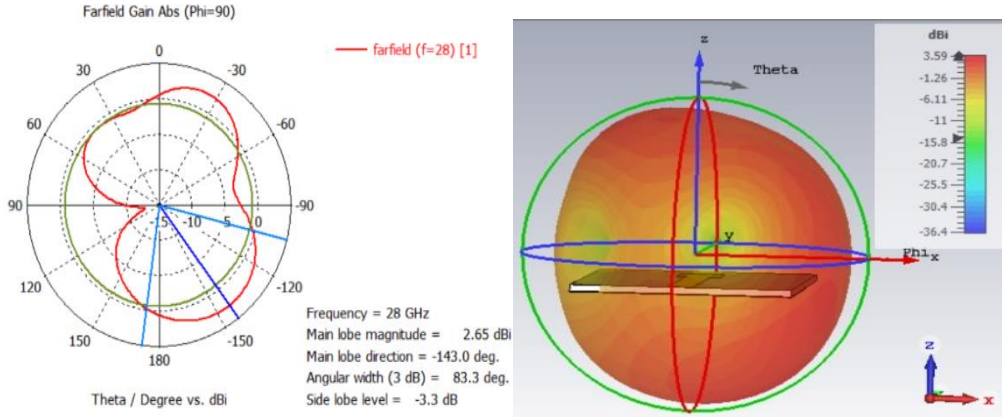

(a) (b)

Figure 5. Radiation pattern (a) 2-D and (b) 3-D

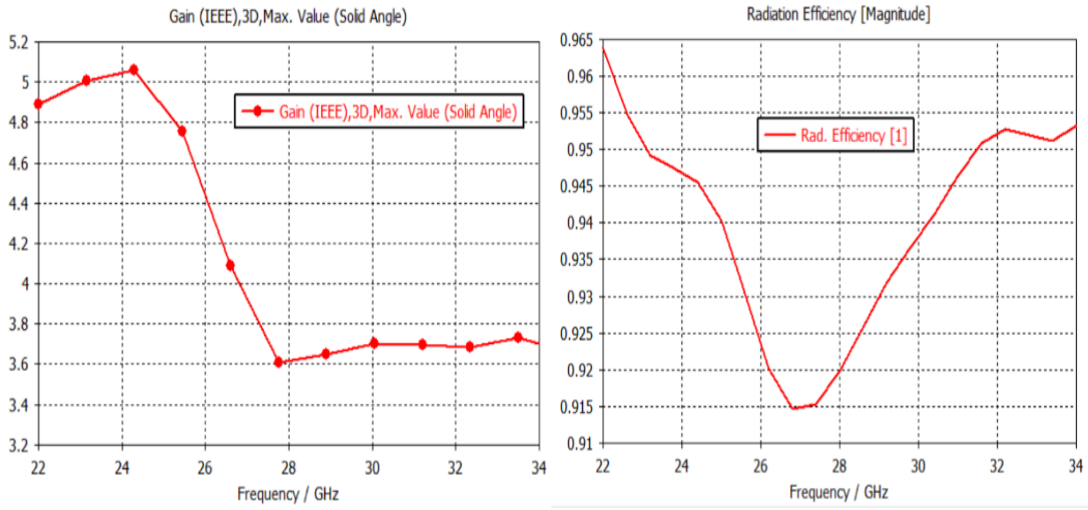

(a) (b)

Figure 6. (a) Gain vs Frequency and (b) Efficiency

2.2 2x1 Array antenna Transformation

In order to Increase the gain at the chosen frequency of interest from 3.59, it is accomplished by transforming the suggested antenna design into a network using corporate feeding, consisting of two antenna elements known as 2x1 array. The primary 50 Ω feed is split into 100 Ω track impedance, which results in the transformation of the array network using below equation. In order to achieve an impedance of 50 Ω, the width of the main feed line is modified, whereas the width of the feed line for other transmission lines is adjusted in order to achieve an impedance of 100 Ω. Figure 7 shows the 2x1 array antenna of proposed design using single calculated antenna dimensions. Figure 7 (a) shows top view and figure 7(b) shows bottom view of proposed array. Using the same dimensions of single antenna element, the division of power for array are optimized. Table 3 explains the calculated and optimized dimensions of proposed 2x1 array. [6] [1] [29] [30]

$$W_z = \left(\frac{377}{zo\sqrt{\varepsilon_r}} - 2\right) \text{x } h_s; W_z = \left(\frac{377}{100\sqrt{2.2}} - 2\right) \text{X } 0.254$$

$$W_{50}=0.78 \text{ mm}; W_{100}=0.22 \text{ mm}$$

Table 3. Calculated and optimized values of 2x1 array

Impedances (Ω)	Calculated	Optimized
50	0.78	0.9
100	0.22	0.28

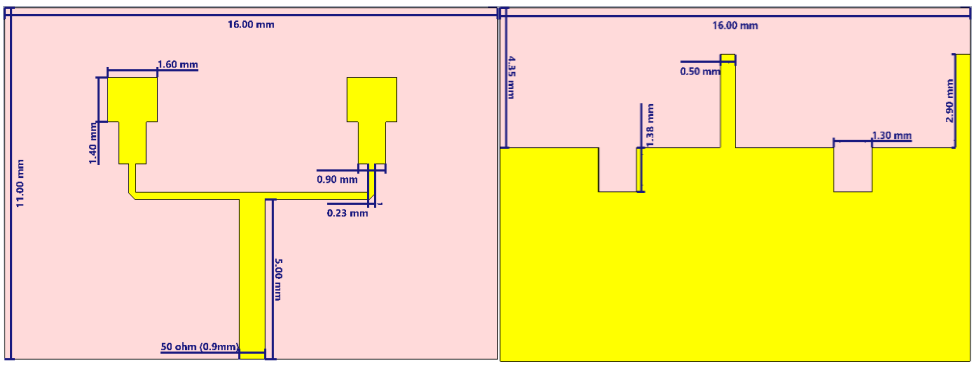

(a) (b)

Figure 7. Proposed 2x1 array (a) Top view and (b) Bottom view

An optimized diemensions for W**50** comes to 0.9mm and W**100** comes to 0.28 mm are listed in table 2. Figure 8 (a) shows the reflection co-efficient and figure 8 (b) shows VSWR of optimized 2x1 array. From the figure it can be observed that it is resonating from 22.6 -- >34 GHz achieveing an impedance bandwidth of >12 GHz with a return loss of -54.5 dB. From figure 8 (b) it can be shown that VSWR value is below 2dB throughout the operating band.

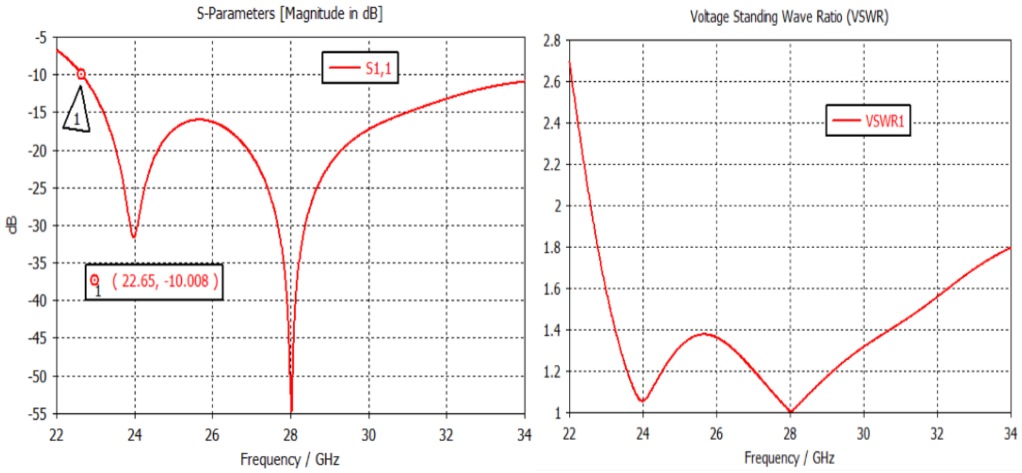

(a) (b)

Figure 8. Simulated results of 2x1 array (Optimized): (a) Return loss and (b) VSWR

Simulated 2-D and 3-D radiation pattern of 2x1 array antenna are depicted in figure 9. Using array arrangements, the single antenna element gain is improved from 3.59 to 7 dBi at a resonance frequency of 28 GHz as shown in figure 9(b).

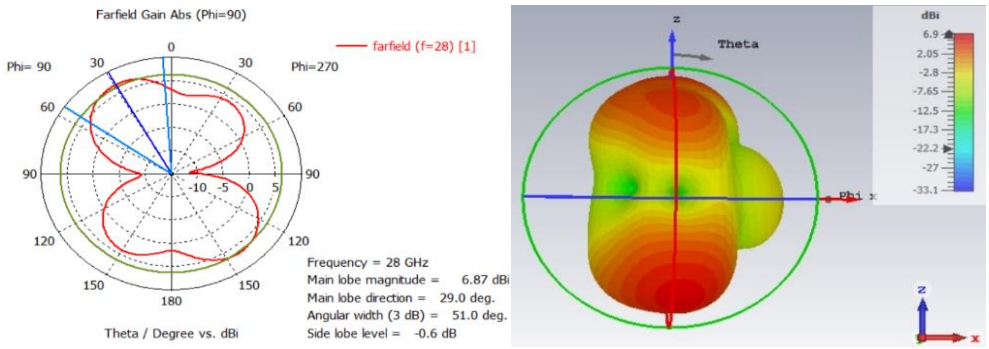

(a) (b)

Figure 9. Simulated radiation pattern of 2x1 array (a) 2-D and (b) 3-D

Gain vs frequency and radiation efficiency of proposed 2x1 array are depicted in figure 10. Figure 10 (a) shows the simulated gain of 2x1 array. From figure 10(a) it can be seen that the proposed 2x1 array achieved a gain of 6.9 dBi with a peak value of 7.82 dBi. Figure 10 (b) indicates efficiency of 2x1 array. It is observed that the array has achieved an efficiency of 93 % at a resonating frequency.

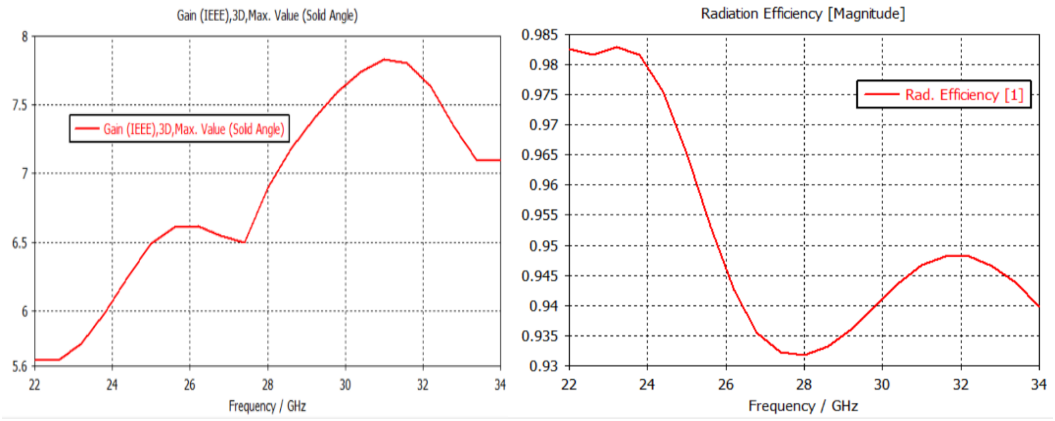

(a) (b)

Figure 10. Simulated results of 2x1 array: (a) Gain vs frequency and (b) Radiation efficiency

2.3 4x1 Array antenna Transformation

For gain enhancement and performance, the two 2x1 array connected in parallel to make 4x1 array and to divide equal power between all ports using equation bellow for impedance calculation. Microstrip feed are used to excite the power divider. The array network is transformed by splitting the main 50 Ω feed into 100 Ω track impedance. If we split the 100 Ω tracks again, we would require a 200 Ω feed line, which is often practically impossible to produce. Instead, we use a quarter wave transformer to match back down to 50 Ω, and then once again split the track into two 100 Ω lines by keeping distance of 0.82λ between each resonator. The main feed line width is adjusted to get an impedance of 50 Ω, while for other transmission lines's feed line width is adjusted to get an impedance of 100 Ω and 70.7 Ω, respectively [6]

The 4x1 array with optimized dimensions is depicted in figure 11. Figure 11 (a) shows top view while figure 11 (b) shows bottom view of proposed 4x1 array. [1]

$$W_{zo} = \left(\frac{377}{zo\sqrt{\varepsilon_r}} - 2\right) \text{x } h_s$$

$$W_z = \left(\frac{377}{50\sqrt{2.2}} - 2\right) \text{X } 0.254$$

W_{50}=0.78 mm

$$W_z = \left(\frac{377}{100\sqrt{2.2}} - 2\right) \text{X } 0.254$$

W_{100}=0.22 mm

$$W_z = \left(\frac{377}{70.7\sqrt{2.2}} - 2\right) \text{X } 0.254$$

$W_{70.7}$=0.45 mm

Table 4. Calculated and optimized dimensions

Impedances (Ω)	Calculated (mm)	Optimized (mm)
50	0.78	0.87
100	0.22	0.28
70.7	0.45	0.362

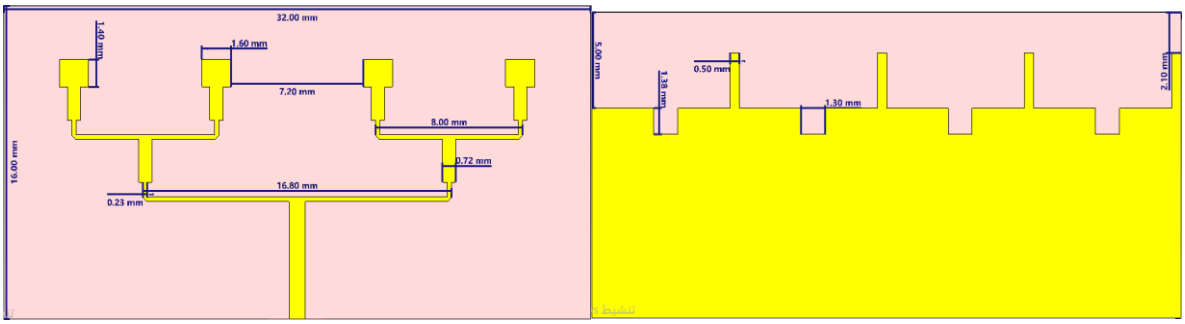

(a) (b)

Figure 11. Proposed 4x1 array Design: (a) Top view and (b) Bottom view

Figure 12 shows the simulated results of proposed array design. Figure 12(a) shows return loss and figure 12 (b) VSWR. From figure 12(a) it can be shown that antenna has dual band resonance of 20.5 – 22.6 GHz and 24.8 – 32.5 GHz covering a wide impedance bandwidth of 2.1 GHz and 9.3 GHz respectively, with a return loss of -61 dB at 27.9 GHz. Minor deviation of resonance from 28 GHz is due to array arrangements. Figure 12 (b) shows VSWR of proposed design. From figure it can be shown that it has a VSWR less than 2 throughout the operating band validates the design accuracy.

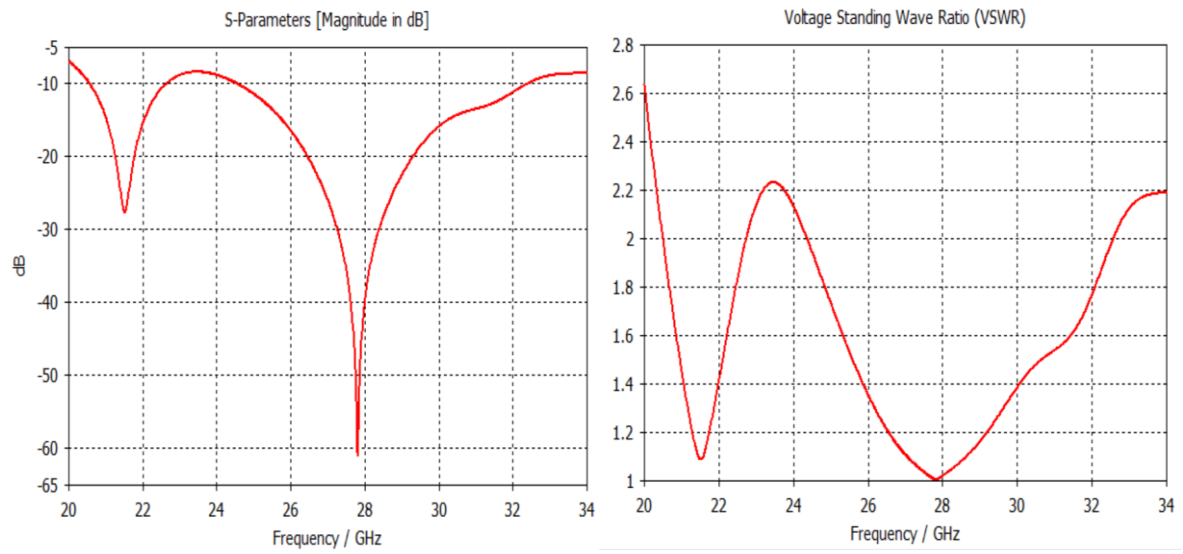

(a) (b)

Figure 12. Simulated Results: (a) Return loss and (b) VSWR

Figure 13 shows the simulated 2-D and 3-D radiation pattern of 4x1 array. From figure it can be shown that the 4x1 array has improved gain of 9.04 dBi with wideband band directivity. Simulated Gain vs frequency and efficiency of proposed 4x1 are depicted in figure 14. From fig 14(a), it can be observed that gain has increased in higher operating band having a value of 9.2 dBi gain at 27.9 GHz. Throughout the operating band, the 4x1 array has an efficiency of more than 93 %. Overall, the performance table of proposed single, 2x1 and 4x1 antenna array elements are listed in table 6.

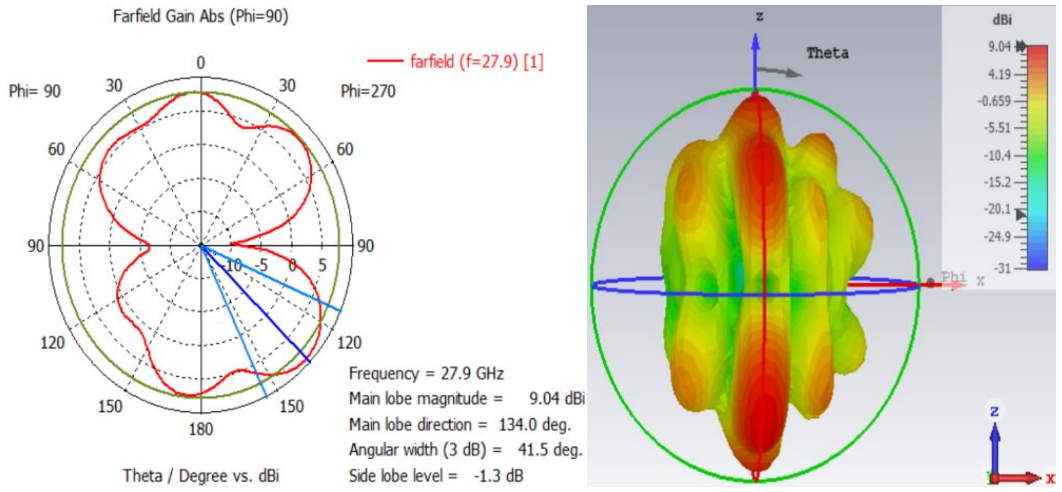

(a) (b)

Figure 13. Simulated Gain of 4x1 array :(a) 2-D and (b) 3-D

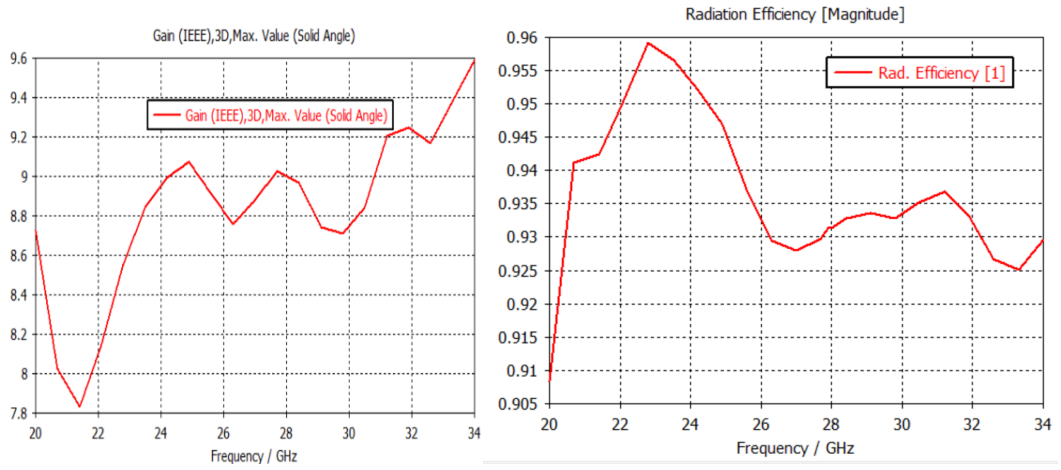

(a) (b)

Figure 14. Simulated results of 4x1 array: (a) Gain vs frequency and (b) Efficiency

3. Single Circular Patch Design

A single circular patch Design is composed of metal with a standard thickness of 0.035 mm, and Roggers RT 5880 serves as the substrate material with a standard height of 0.254 mm. The substrate dimensions are 8x8 mm² with a circular radius of 1.9 mm, determined using equation (8---13). For impedance matching, the microstrip feed line is designed to have a 50 Ω impedance. The feed line has a width of 0.80 mm and a length of 3.26 mm. Figure 15 provides the top and back views of the single microstrip circular patch design, with Figure 15 (a) illustrating the top view, and Figure 15 (b) showcasing the back view. [1] [29] [30]

Circular patch antenna radius

$$R = \frac{F}{\sqrt{1+\frac{2h}{\pi\epsilon_r F}\left[ln\left(\frac{\pi F}{2h}+1.7726\right)\right]}} \tag{8}$$

Where $F = \frac{8.791\ X\ 10^9}{fr}$ (9)

$$F` = \frac{8.791\ *10^9}{28*10^9} = 0.313$$

$$R = \frac{0.313}{\sqrt{1+\frac{2*0.254}{0.314*2.2*0.313}\left[ln\left(\frac{3.14*0.313}{2*0.254}+1.7726\right)\right]}}$$

$$R = 1.973mm$$

The Effective length L*eff* of patch is:

$$L_{eff} = L + 2\Delta L \tag{10}$$

Because of fringing fields, the length is changed and is assumed by:

$$\frac{\Delta L}{h} = 0.412\frac{(\epsilon_{eff}+0.3)(\frac{W}{h}+0.264)}{(\epsilon_{eff}-0.258)(\frac{W}{h}+0.8)} \tag{11}$$

$$\Delta L = 0.254\left[0.412\frac{(2.05+0.3)(\frac{4.23}{0.254}+0.264)}{(2.05-0.258)(\frac{4.23}{0.254}+0.8)}\right] = 0.523$$

$$L_{eff} = 3.466 + 2*0.523 = 4.5\ \text{mm}$$

the substrate length (Ls) and width (Ws) are:

$$W_s = 2\ (Patch\ diameter) \quad (12)$$

= 2 (2*R) =2(2 * 1.9)=7.6mm

$$L_s = 2\ (Patch\ diameter) \quad (13)$$

= 7.6mm

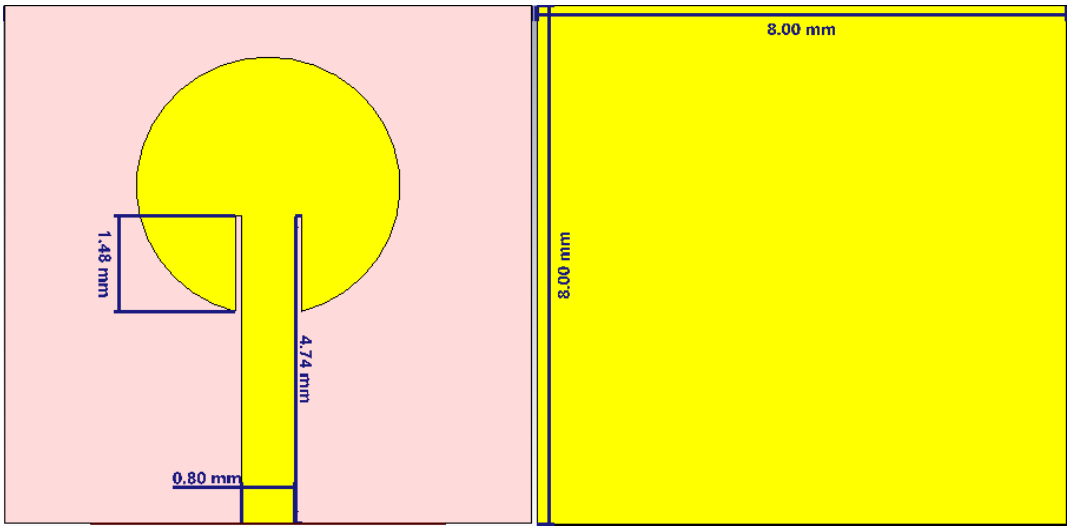

(a) (b)

Figure 15. Simple circular Microstrip patch antenna: (a) top view and (b) bottom view

Simulated S11 of single circular patch design are depicted in figure 16. The figure shows that it does not resonate at the operating frequency required for this project. After going through with the optimization process using the CST® software package, the final optimum parameters for the single circular microstrip patch antenna as mentioned in the subsequent section.

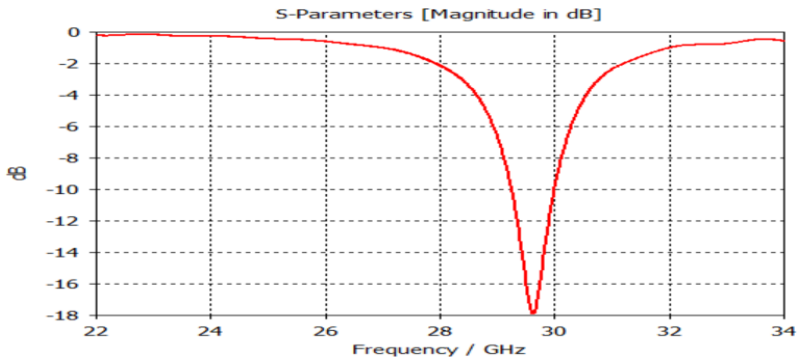

Figure 16. The return loss of Single Circular Patch Design

3.1 Improved Single Circular Patch Design

This section explains the most compact and modified antenna in order to improve bandwidth, efficiency and gain and other performances. In order to improve the performance of single Circular patch Antenna, a truncation ground also known as partial ground are introduced at the bottom of substrate to fulfill the 5G requirements. Moreover, a rectangular slot is introduced in the mid of partial ground of 1.38 x 1.3 mm^2 dimension and extra vertical strip at the top right corner of partial ground. The top and back view of improved single circular patch design are depicted in fig 17(a) and (b) respectively. dimension of single Circular patch design is listed in table 5. [1] [29] [30] [25]

Table 5: calculated and optimization values of Single Circular Patch Design

Parameter	Calculated value (mm)	Improved Values(mm)
F_r	28 GHz	28 GHz
Feed width (wf)	0.8	0.9
Feed Length (Lf)	3.26	5
Patch radius (a)	1.9	1.3

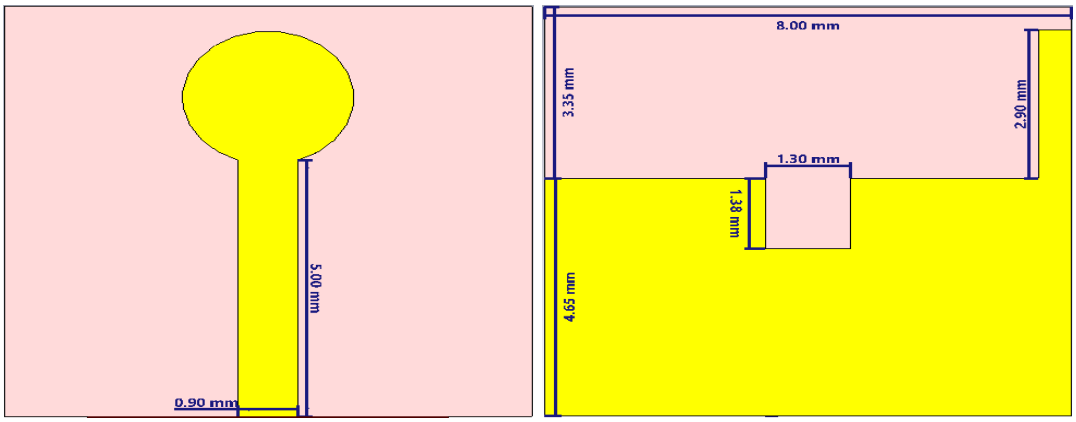

(a) (b)

Figure 17. Single antenna element: (a) Top view and (b) Bottom view

Figure 18 (a) displays the simulated return loss of this design. The antenna exhibits resonance at 28 GHz with a return loss of -36.2 dB and a bandwidth extending from 25.8 to more than 34 GHz, achieving a bandwidth of more than 9 GHz. Figure 18 (b) depicts the VSWR of this design, showcasing that the antenna maintains a VSWR below 2 dB throughout the operating band, confirming the validation of the design. The radiation pattern 2D and 3D of the proposed design is simulated at 28 GHz, as depicted in Figure 19. Figure 19 (a) shows a 2D radiation pattern indicating wideband radiation in all directions with a simulated beamwidth of 84.7 degrees. Figure 19 (b) shows the 3D radiation pattern of the proposed design at the central frequency of 28 GHz. Simulated gain versus frequency and efficiency of the proposed design are shown in Figures 20 (a) and (b), respectively. From Figure 20 (a), it is evident that the antenna has a gain of 3.61 dBi at 28 GHz and a peak gain of 4.4 dBi at 26 GHz, maintaining more than 3.6-4.4 dBi gain across the bandwidth. Figure 20 (b) explains the simulated radiation efficiency of the proposed design. As shown in the figure, the antenna has an efficiency of 92% at the lower frequency range, and efficiency increases gradually at the higher frequency band.

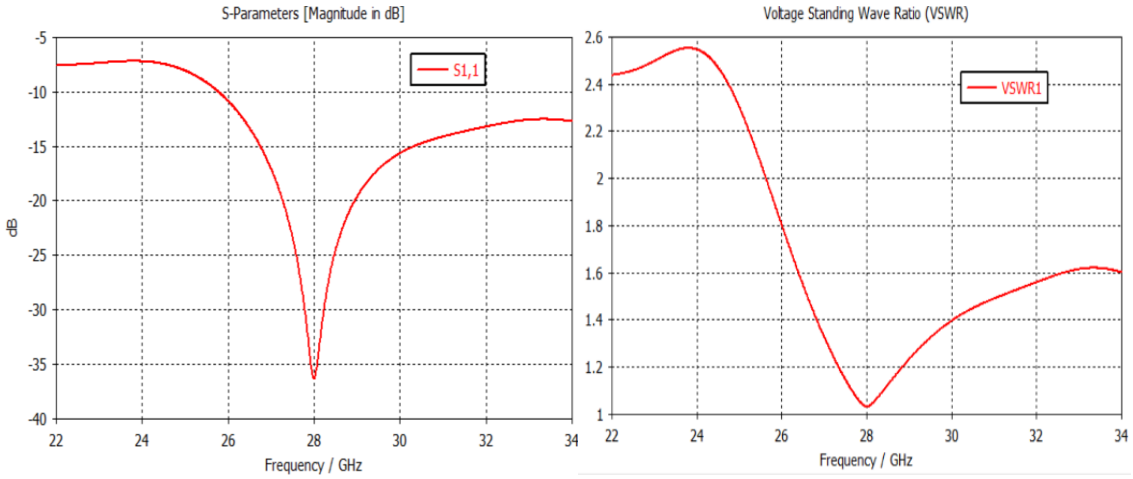

(a) (b)

Figure 18. (a) S11 of proposed optimized single circular antenna element and (b) VSWR

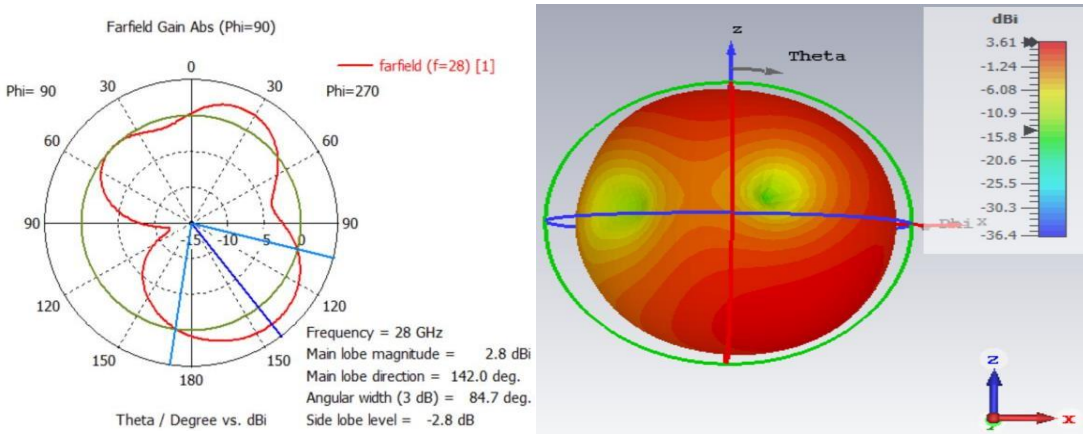

(a) (b)

Figure 19. Radiation pattern (a) 2-D and (b) 3-D

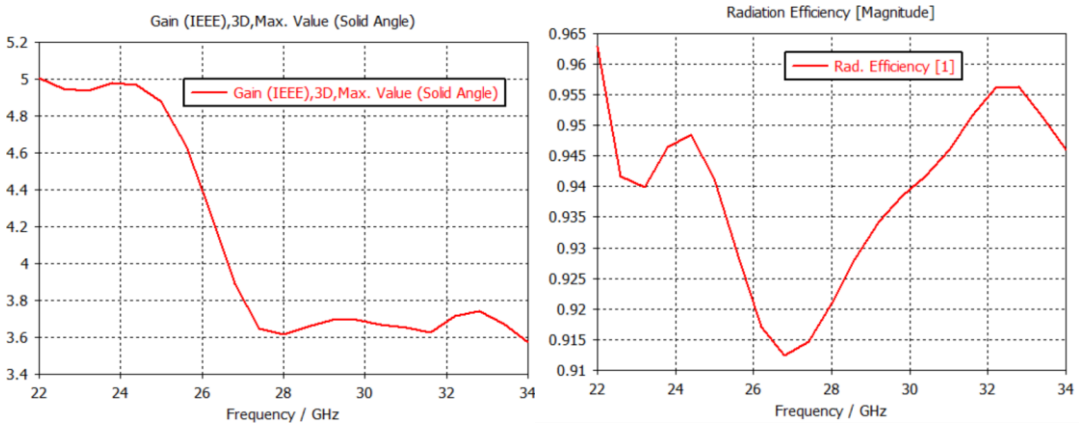

(a) (b)

Figure 20. (a) Gain vs Frequency and (b) Efficiency

3.2 2x1 Microstrip Circular Patch Array

To enhance gain and other performance, the single circular patch is extended to a 2x1 microstrip circular patch array, as shown in Figure 21. Figure 21(a) shows the front view, while Figure 21(b) shows the back view. The total dimensions of the 2x1 array are 11 x 16 mm^2. Partial ground is used at the bottom level of the substrate with a slot and vertical strip. Simulated return loss of the proposed design is shown in Figure 22 (a). The antenna has a return loss of -56.6 dB with a wide bandwidth of 6.5 GHz, resonating from 25.2 to 31.7 GHz. Figure 22 (b) shows the VSWR of the proposed 2x1 array. From the figure, it can be seen that it has a VSWR less than 2 dB throughout the operating band, validating the design.
The 2D and 3D Radiation patterns of the 2x1 array antenna are depicted in Figure 23. The gain of a single antenna element is improved from 3.61 dBi to 7.06 dBi using array arrangements.

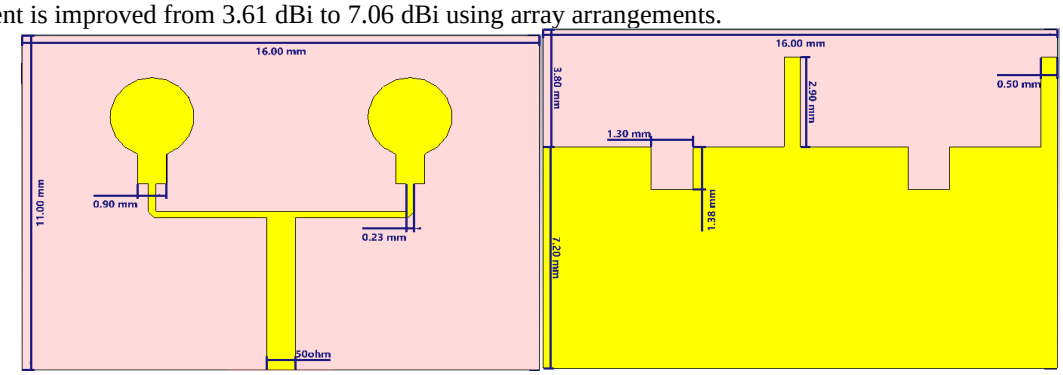

(a) (b)

Figure 21. Proposed 2x1 array: (a) Top view and (b) Bottom view

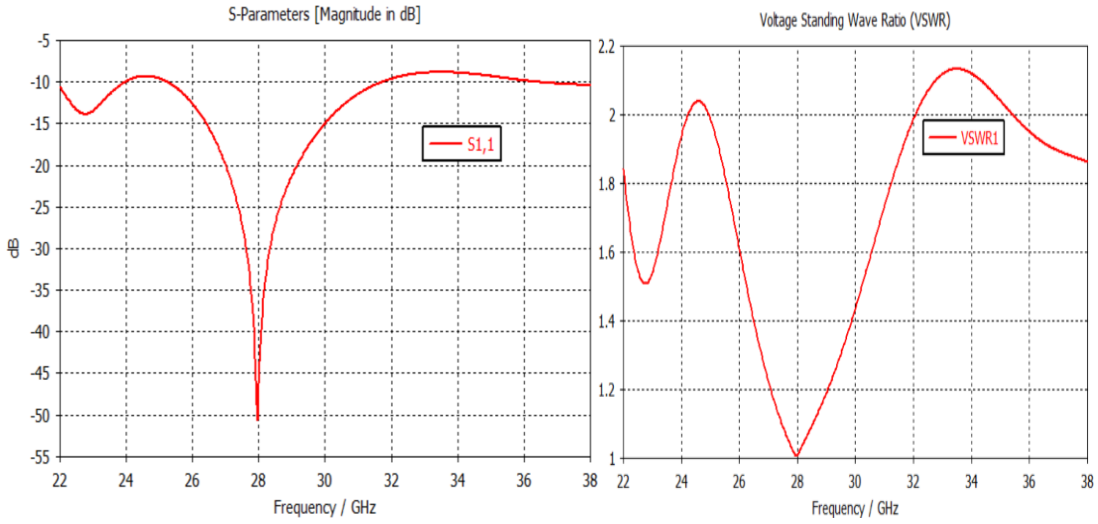

(a) (b)

Figure 22. Simulated results of 2x1 array (Optimized): (a) Return loss and (b) VSWR

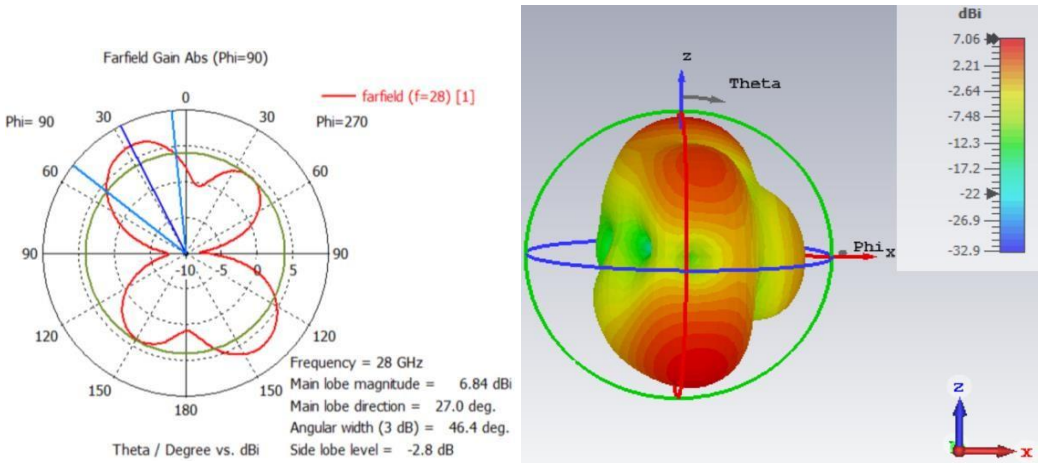

(a) (b)

Figure 23. Simulated radiation pattern of 2x1 array :(a) 2-D and (b) 3-D

Figures 24 (a) and 24 (b) shows gain versus frequency and radiation efficiency of the proposed design, respectively. From Figure 24 (a), it can be observed that gain is increasing at the higher frequency band and achieved a peak gain of 7.88 dBi at 31 GHz. Furthermore, the efficiency at higher frequency is more than 95% with higher efficiency of 97% at 31 GHz, as shown in Figure 24 (b). These results validate the design efficiency and performance.

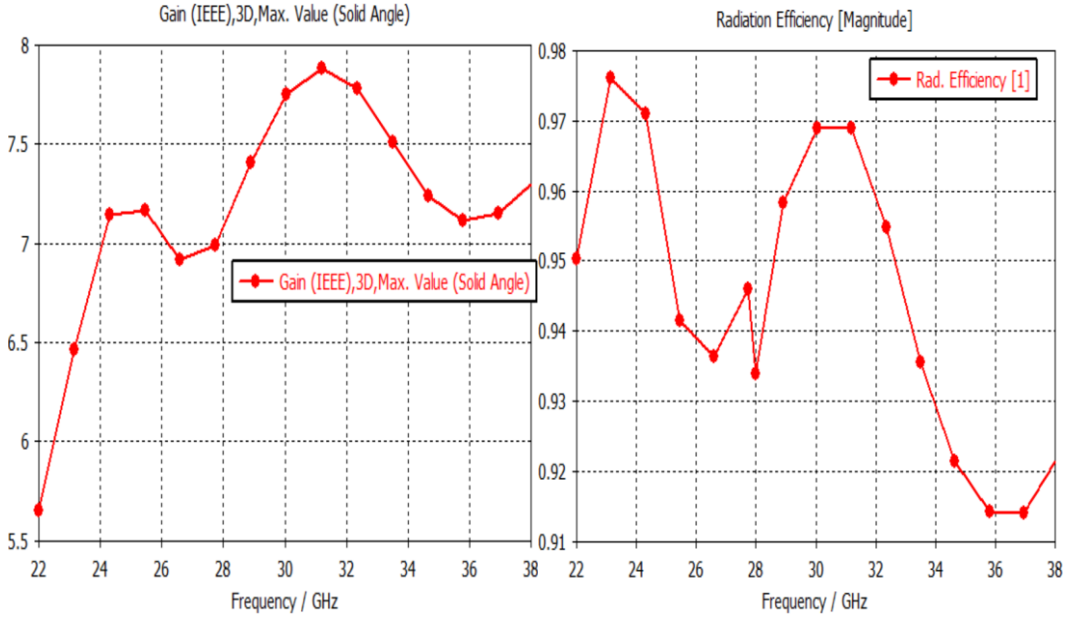

(a) (b)

Figure 24. Simulated results of 2x1 array: (a) Gain vs frequency and (b) Radiation efficiency

3.3 4x1 Microstrip Circular Patch Array

For gain enhancement and improved performance, two 2x1 arrays are connected in parallel to form a 4x1 array. The array network undergoes transformation by splitting the main 50 Ω feed into 100 Ω track impedance. To avoid the impracticality of producing a 200 Ω feed line by splitting the 100 Ω tracks again, a quarter-wave transformer is employed to match back down to 50 Ω. Subsequently, the track is split into two 100 Ω lines with a distance of 0.8λ between each resonator.

The main feed line width is adjusted to achieve an impedance of 50 Ω, while the feed line width for other transmission lines is adjusted to obtain impedances of 100 Ω and 70.7 Ω, respectively. The 4x1 array is depicted in Figure 25, where (a) represents the top view and (b) illustrates the back view of the 4x1 array.

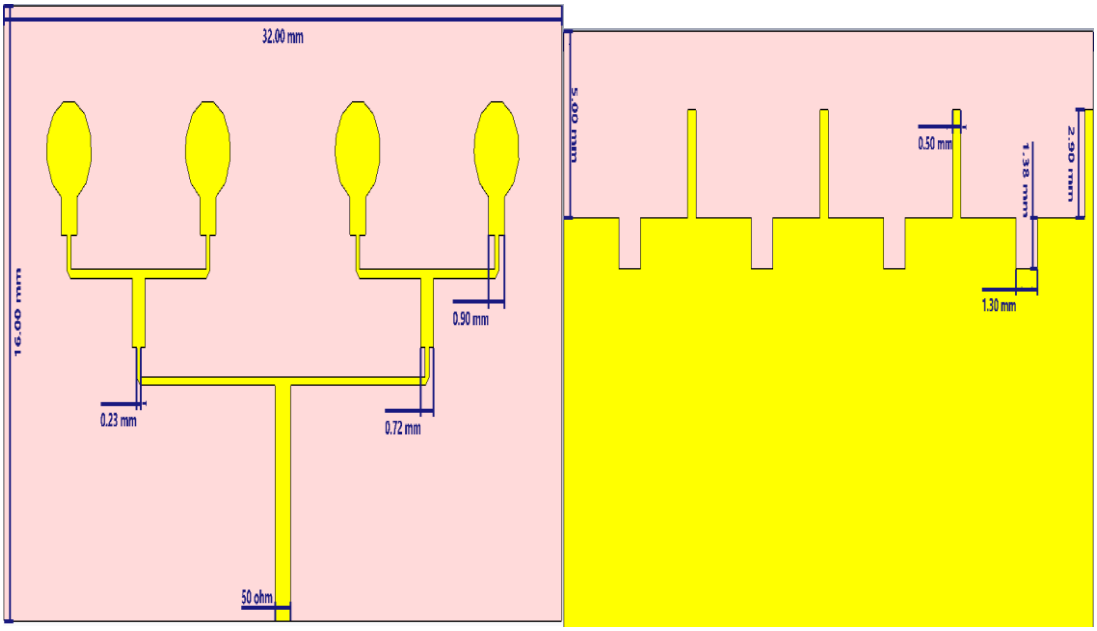

(a) (b)

Figure 25. Proposed 4x1 array Design: (a) Top view and (b) Bottom view

Figure 26 present simulated return loss and VSWR of the 4x1microstrip circular patch array design, respectively. From figure 26 (a), it can be observed that the antenna has a return loss of -35 dB with a wide bandwidth of 8 GHz resonating from 25 GHz to 33 GHz. Figure 26 (b) expresses VSWR of the 4x1 array, which remains below 2 dB throughout the operating band. These results validate the design and confirm its applicability for upcoming 5G applications.

Figure 27 presents the 2D and 3D far field radiation pattern of the 4x1 microstrip circular patch array. From figure 27 (a), it can be seen that it has a wide radiation pattern in all directions with a gain of 9.05dBi and a 134-degree main lobe angle direction. Gain versus frequency and efficiency of the 4x1 array are depicted in figure 28. From figure 28 (a), it can be shown that the gain is increasing gradually from the lower to higher operating band, achieving a peak gain of 9.6dBi at 31.2 GHz. Figure 28 (b) expresses the simulated efficiency of the 4x1 circular patch array, having more than 93% throughout the operating band, with a peak efficiency of 94%. High gain with high efficiency validates the design performance and its application. The circular antenna design performance is listed in table 7.

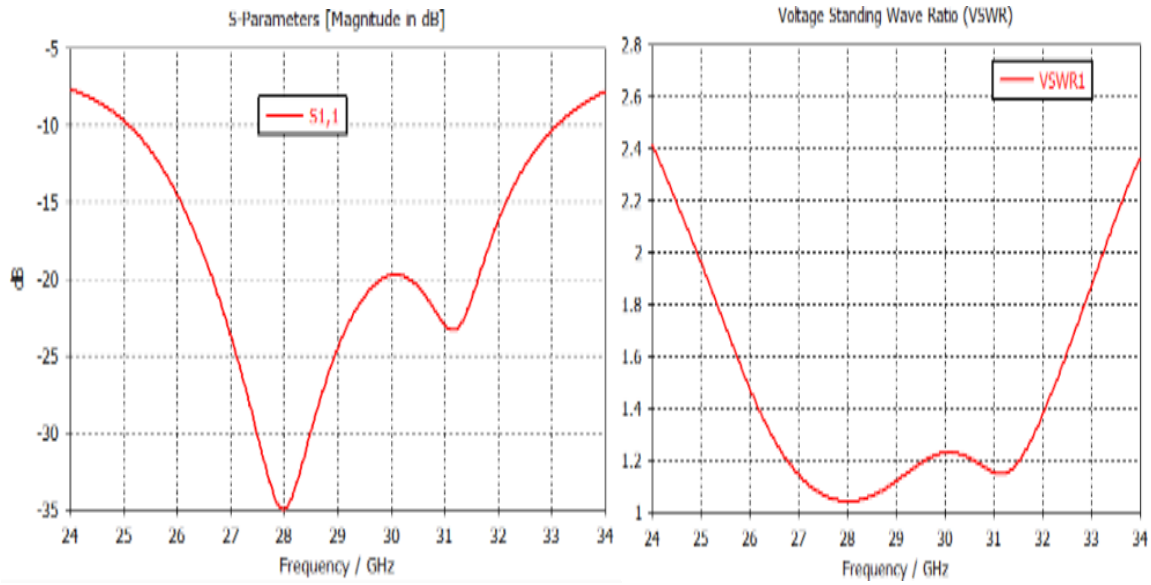

(a) (b)

Figure 26. Simulated Results: (a) Return loss and (b) VSWR

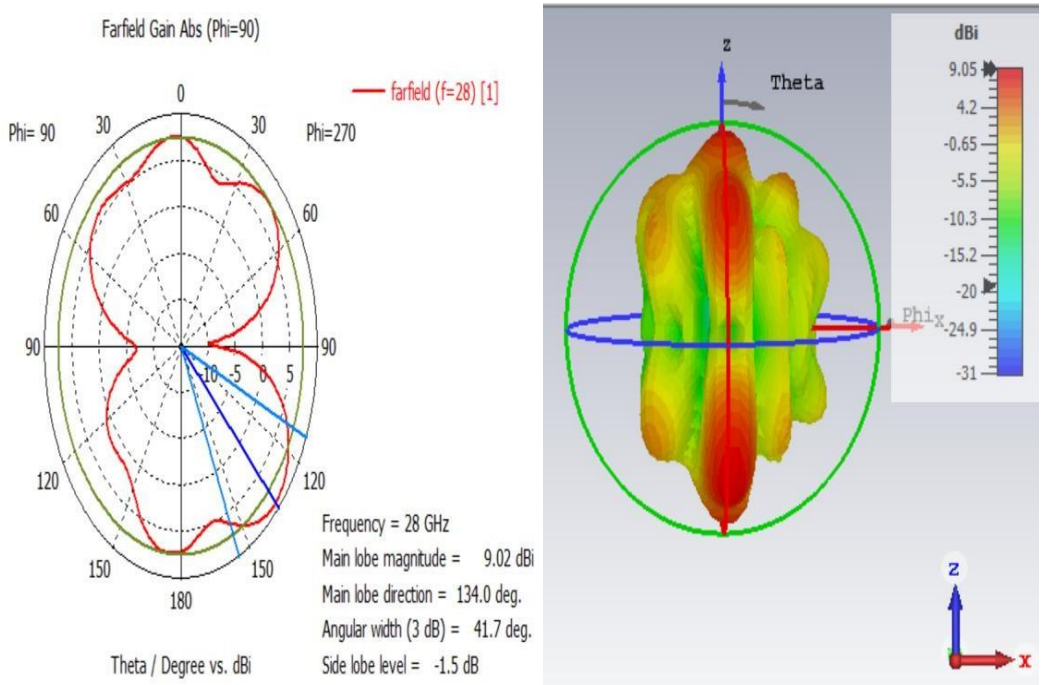

(a) (b)

Figure 27. Simulated Gain of 4x1 array :(a) 2-D and (b) 3-D

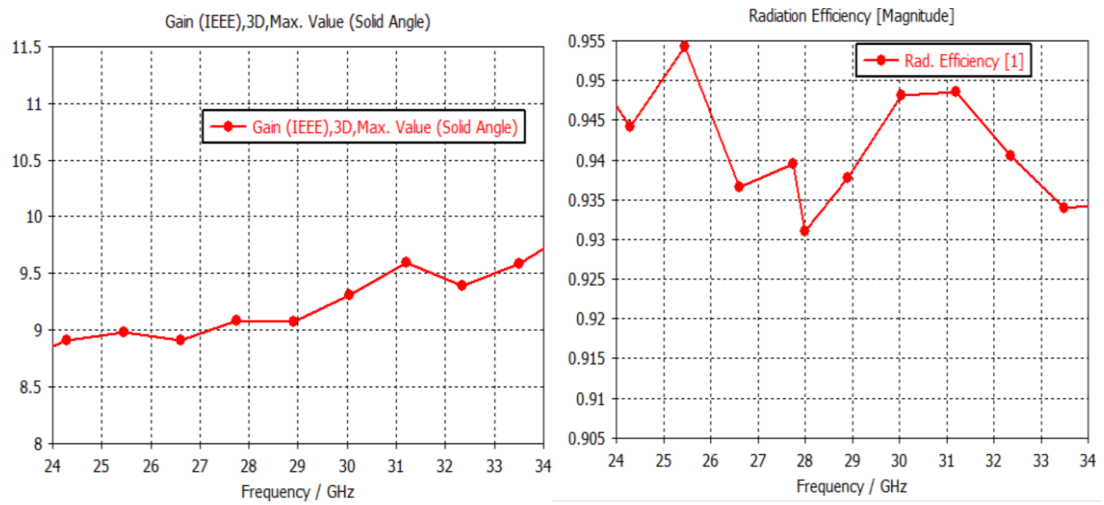

(a) (b)

Figure 28. Simulated results of 4x1 array: (a) Gain vs frequency and (b) Efficiency

4. Analysis and Discussion

Tables 6 and 7 summarizes the performance of the proposed antennas, all operating in the 28 GHz band. They exhibit good impedance matching with return loss levels below -10 dB at 28 GHz. However, there is a relatively undesirable return loss at frequencies outside the operating frequency range. This can be compensated by the value of the return loss at the operating frequency, which is much lower than -10 dB. Therefore, some applications may prioritize values significantly lower than -10 dB at the operating frequency, regardless of the return loss outside the operating range. In general, the difference in patch shape does not constitute a significant distinction in terms of results, as the simulation outcomes are almost similar. The directivity increases with the number of patches, and the 4x1 array exhibits the highest directivity and gain. Hence, it is deemed the most suitable for 5G wireless communications.

Table 6: Performance table of proposed design of rectangular patch

Antenna type	size (mm^2)	Fr (GHz)	S_{11} (dB)	Bandwidth (GHz)	Gain (dBi)	Directivity (dBi)	Efficiency (%)
Single	8x8	28	-56.6	>9.6	3.59	3.91	91
2x1	16x11	24 , 28	-32 ,-54.5	> 12.6	7	7.2	>93
4x1	30x16	21.5 , 27.9	-27 , -61	2.1, 9.3	9.04	9.35	>94

Table 8 provides a detailed comparison between the proposed design and recently published woks. This comparison highlights several key parameters, including the number of antenna elements, return loss, bandwidth, gain, directivity, and efficiency. The results clearly indicate that this design offers a miniaturized size while maintaining excellent performance. The antenna's compact electrical and physical dimensions, relative to existing works, underscore its potential for seamless integration into devices intended for 5G applications.

Table 7: Performance table of proposed design of circular patch

Antenna type	size (mm^2)	Fr (GHz)	S_{11} (dB)	Bandwidth (GHz)	Gain (dBi)	Directivity (dBi)	Efficiency (%)
Single	8x8	28	-36.2	8.6	3.61	3.98	91
2x1	16x11	28	-50.6	6.5	7.06	7.36	93.5
4x1	32x16	28	-35	8	9.05	9.35	94.5

Table 8: Comparison of the proposed design with recently published works

Antenna type		Number of antenna	Fr (GHz)	S_{11}(dB)	Bandwidth (GHz)	Gain (dBi)	Directivity (dBi)	Efficiency (%)
[22]		1x6	28	-30.70	4.63	7.47	--	--
[23]		1	28	-35	--	3.77	--	--
[24]		13	28	-22	0.9	8.42	--	93
[25]		2x1	28	-35.91	1.43	9.42	9.5	>99.8
[26]		1x4	28	-17	--	--	6.92	--
[27]		1x4	28	-30.71	2.68	--	9.87	
[28]		1	28	-25	0.55	4.78	--	--
This work	Rectangular	1	28	-56.6	>9.6	3.59	3.91	91
		2x1	24 , 28	-32 ,-54.5	> 12.6	7	7.2	>93
		4x1	21.5 , 27.9	-27 , -61	2.1, 9.3	9.04	9.35	>94
	Circular	1	28	-36.2	8.6	3.61	3.98	91
		2x1	28	-50.6	6.5	7.06	7.36	93.5
		4x1	28	-35	8	9.05	9.35	94.5

5. Conclusion

This paper presents the calculations and simulations of the proposed antennas. The three proposed antennas were simulated in the 3-D solver of CST. Dimensions have been optimized through the CST package to achieve a trade-off between the smallest size and the best possible performance. The proposed antennas provide good impedance matching, radiation patterns and gain.

The design and analysis of microstrip patch antennas, including single rectangular patches and patch arrays, demonstrate their potential for 5G wireless communication applications. The transformation of a single antenna design into 2x1 and 4x1 arrays shows significant improvements in gain, efficiency, and bandwidth, making them suitable for upcoming 5G applications. The simulation results validate the accuracy and applicability of the proposed designs, paving the way for enhanced wireless communication systems. Additionally, the high radiation efficiency and consistent gain across the operating bandwidth further underscore the effectiveness of these antenna configurations. Overall, this work contributes valuable insights into the design methodology and analysis of microstrip patch antennas for advanced wireless communication technologies.

Refrences

[1] Balanis, C.A., Antenna Theory: Analysis and Design, John Wiley& Sons.
[2] D. N. Arizaca-Cusicuna, J. Luis Arizaca-Cusicuna and M. ClementeArenas, "High Gain 4x4 Rectangular Patch Antenna Array at 28GHz for Future 5G Applications," 2018 IEEE XXV International Conference on Electronics, Electrical Engineering and Computing (INTERCON), Lima, 2018, pp. 1-4.
[3] Y. Rahayu and M. I. Hidayat, "Design of 28/38 GHz Dual-Band Triangular-Shaped Slot Microstrip Antenna Array for 5GApplications," 2018 2nd International Conference on Telematics and Future Generation Networks (TAFGEN), Kuching, 2018, pp. 93-97
[4] Zia Ullah Khan, Qammer H. Abbasi, Angel Belenguer, Tian Hong Loh, and Akram Alomainy , "Empty Substrate Integrated Waveguide Slot Antenna Array for 5G Applications," 2018 International Conference on Intelligent Systems and Computer Vision (ISCV), Fez, 2018, pp. 1-4
[5] J. Tan, S. Gong and W. Jiang, "A Novel Connected PIFA Array With MIMO Configuration for 5G Mobile Applications," 2018 Sixth AsiaPacific Conference on Antennas and Propagation (APCAP), Xi'an, 2018, pp. 1-3.
[6] Mohammad S. Sharawi and Muhammad Ikram "Slot Based Connected Antenna Arrays for 5G Mobile Terminals," in Communications Magazine, IEEE , vol.52, no.2, pp.106-113, February 2018.
[7] Zhang, S.; Chen, X.; Syrytsin, I.; Pedersen, G.F. A Planar Switchable 3-D-Coverage Phased Array Antenna and Its User Effects for 28-GHz Mobile Terminal Applications. IEEE Trans. Antennas Propag. 2017, 65, 6413–6421
[8] M. S. Ibrahim, "High Gain 4x4 Rectangular Patch Antenna Array at 28 GHz for Future 5G Applications," 2018 International Applied Computational Electromagnetics Society Symposium (ACES), Denver, CO, 2018, pp. 1-2.
[9] D. Mungur and S. Duraikannan, "Design and Analysis of 28 GHz Millimeter Wave Antenna Array for 5G Communication Systems", Journal of Science Technology Engineering and Management-Advanced Research & Innovation, vol. 1, no. 3, p. 10, 2018. [Accessed 10 September 2019].
[10] Surendran Subramanian, Veeraiyah Thangasamy. „" Modified Triple Band Microstrip Patch antenna for Higher 5G bands, In AEEICB-18
[11] Gampala, G, and Reddy, C. J., "Design of Milimeter Wave Antenna Arrays for 5G Cellular Applications using FEKO," IEEE International Conference on Wireless Information Technology and System (ICWITS) and Applied Computational Electromagnetics (ACES), 2016.
[12] Hasan, M.M.; Faruque, M.R.I.; Islam, M.T. Dual band metamaterial antenna for LTE/bluetooth/WiMAX system. Sci. Rep. 2018, 8, 1240.
[13] Y. Zhang, J.-Y. Deng, M.-J. Li, D. Sun, and L.-X. Guo, ''A MIMO dielectric resonator antenna with improved isolation for 5G mm-wave applications,'' IEEE Antennas Wireless Propag. Lett., vol. 18, no. 4, pp. 747–751, Apr. 2019.
[14] F. Wang, Z. Duan, X. Wang, Q. Zhou, and Y. Gong, ''High isolation millimeter-wave wideband MIMO antenna for 5G communication,'' Int. J. Antennas Propag., vol. 2019, pp. 1–12, May 2019.
[15] N. Hussain, M.-J. Jeong, J. Park, and N. Kim, ''A broadband circularly polarized Fabry–Pérot resonant antenna using a single-layered PRS for 5G MIMO applications,'' IEEE Access, vol. 7, pp. 42897–42907, Apr. 2019.
[16] N. Shoaib, S. Shoaib, R. Y. Khattak, I. Shoaib, X. Chen, and A. Perwaiz, ''MIMO antennas for smart 5G devices,'' IEEE Access, vol. 6, pp. 77014–77021, Oct. 2018.
[17] H. Piao, Y. Jin, and L. Qu, ''A compact and straightforward selfdecoupled MIMO antenna system for 5G applications,'' IEEE Access, vol. 8, pp. 129236–129245, Jul. 2020.
[18] Z. Wani, M. P. Abegaonkar, and S. K. Koul, ''A 28-GHz antenna for 5G MIMO applications,'' Prog. Electromagn. Res. Lett., vol. 78, pp. 73–79, Mar. 2018.
[19] Z. Kordiboroujeni and J. Bornemann, ''Designing the width of substrate integrated waveguide structures,'' IEEE Microw. Wireless Compon. Lett., vol. 23, no. 10, pp. 518–520, Oct. 2013.
[20] X. Chen, S. Zhang, and Q. Li, ''A review of mutual coupling in MIMO systems,'' IEEE Access, vol. 6, pp. 24706–24719, Apr. 2018.
[21] Rappaport, T.S.; Sun, S.; Mayzus, R.; Zhao, H.; Azar, Y.; Wang, K.; Wong, G.N.; Schulz, J.K.; Samimi, M.; Gutierrez, F. Millimeter wave mobile communications for 5G cellular: It will work! IEEE Access 2013, 1, 335–349.

[22] Y. Rahayu and M. I. Hidayat, "Design of 28/38 GHz dual-band triangular-shaped slot microstrip antenna array for 5G applications," in 2018 2nd International Conference on Telematics and Future Generation Networks (TAFGEN), Jul. 2018, pp. 93–97, doi: 10.1109/TAFGEN.2018.8580487

[23] Ali, Mohamed Mamdouh & Haraz, Osama & Alshebeili, Saleh & Sebak, A.. (2016). Broadband printed slot antenna for the fifth generation (5G) mobile and wireless communications. 1-2. 10.1109/ANTEM.2016.7550106.

[24] C. K. Ali and M. H. Arif, "Dual-band millimeter-wave microstrip patch array antenna for 5G smartphones," in 2019 International Conference on Advanced Science and Engineering (ICOASE), Apr. 2019, pp. 181–185, doi: 10.1109/ICOASE.2019.8723719.Lastname, F. M., F. M. Lastname and F. M. Lastname, "Title of the journal paper," Journal Title Abbreviation, Vol. 34, No. 10, 1064–1076, 1986.

[25]] S.Didi , I.Halkhams , A.Es-Saqy , M.Fattah , Y Balboul , S mazer and M. El Bekkali "New microstrip patch antenna array design at 28 GHz millimeter-wave for fifth-generation application,"IJECE Vol. 13, No. 4, August 2023, pp. 4184~4193

[26] T. Zafar, A. Noor, T. Ahmed, N. M. J. Piya, and A. K. M. A. M. Azad, "Development and Study of 28GHz Antenna for Different Shapes and Work on Antenna Transparency for Celluler Devices," in 2020 IEEE Region 10 Symposium (TENSYMP), 2020, doi: 10.1109/tensymp50017.2020.9230779

[27] Musa, Umar & Babani, Suleiman & Babale, Suleiman & Ali, Abubakar & Yunusa, Zainab & Halliru Lawan, Sani. (2023). Bandwidth enhancement of millimeter-wave microstrip patch antenna array for 5G mobile communication networks. Bulletin of Electrical Engineering and Informatics. 12. 2203-2211. 10.11591/eei.v12i4.4680.

[28] ENIS KOBAL 1, RUI-JIA LIU[2], CHAO YU[2] , AND ANDING ZHU[1], A High Isolation, Low-Profile, Triple-Port SIW Based Annular Slot Antenna for Millimeter-Wave 5G MIMO Applications

[29] Khouyaoui, Ibrahim & Hamdaoui, Mohamed & Jaouad, Foshi. (2024). Development and Examination of a 2.4 GHz Rectangular Patch Microstrip Antenna Incorporating Slot and Dielectric Superstrates. 10.1007/978-3-031-48573-2_41.

[30] Khouyaoui, Ibrahim & Jaouad, Foshi & Hamdaoui, Mohamed. (2023). Analyzing the Influence of a Superstrate and Slot on a Circular Patch Antenna Operating at 2.4 GHz Resonance Frequency. E3S Web of Conferences. 469. 10.1051/e3sconf/202346900077.

[31] Elalaouy, Ouafae & el Ghzaoui, Mohammed & Jaouad, Foshi. (2024). Mutual Coupling Reduction of a Two-Port MIMO Antenna Using Defected Ground Structure. e-Prime - Advances in Electrical Engineering, Electronics and Energy. 8. 100557. 10.1016/j.prime.2024.100557.

[32] Elalaouy, Ouafae & Varakumari, Samudrala & el Ghzaoui, Mohammed & Jaouad, Foshi & Das, Sudipta. (2023). A Compact Two-port MIMO Array Antenna for ISM/5G NR/WLAN Band Applications. Journal of Nano- and Electronic Physics. 15. 01027-1. 10.21272/jnep.15(1).01027.

[33] L. G. Ayalew and F. M. Asmare, "Design and optimization of pi-slotted dual-band rectangular microstrip patch antenna using surface response methodology for 5G applications," Heliyon, vol. 8, no. 12, p.e12030, Dec. 2022, doi: 10.1016/j.heliyon.2022.e12030

[34] P. Subbulakshmi and R. Rajkumar, "Design and characterization of corporate feed rectangular microstrip patch array antenna," in 2013 IEEE International Conference ON Emerging Trends in Computing, Communication and Nanotechnology (ICECCN), Mar. 2013, doi: 10.1109/ice-ccn.2013.6528560

[35] K. Bangash, M. M. Ali, H. Maab, and H. Ahmed, "Design of a Millimeter Wave Microstrip Patch Antenna and Its Array for 5G Applications," in 2019 International Conference on Electrical, Communication, and Computer Engineering (ICECCE), Jul. 2019,doi:10.1109/icecce472